Colloids and Surfaces B: Biointerfaces 102 (2013) 674–681

Contents lists available at SciVerse ScienceDirect

Colloids and Surfaces B: Biointerfaces

journal homepage: www.elsevier.com/locate/colsurfb

Electrospun Chitosan-graft-PLGA nanofibres with significantly enhanced hydrophilicity and improved mechanical property

Ai.D. Li[a], Z.Z. Sun[a], M. Zhou[a], X.X. Xu[a,c], J.Y. Ma[a], W. Zheng[a,b,*], H.M. Zhou[a], L. Li[a], Y.F. Zheng[a,d]

[a] Center for Biomedical Materials and Engineering, Harbin Engineering University, Harbin 150001, China
[b] Key Laboratory of Superlight Materials and Surface Technology, Ministry of Education, College of Material Science and Chemical Engineering, Harbin Engineering University, Harbin 150001, China
[c] Laboratory for Functional Materials, School of Mechanical and Chemical Engineering, The University of Western Australia, 35 Stirling Highway, Crawley, WA 6009, Australia
[d] Department of Materials Science and Engineering, College of Engineering, Peking University, Beijing 100871, China

ARTICLE INFO

Article history:
Received 14 January 2012
Received in revised form
18 September 2012
Accepted 20 September 2012
Available online 6 October 2012

Keywords:
Chitosan-graft-PLGA
Cross-link
Electrospinning nanofibres
Mechanical property

ABSTRACT

This work reported a novel poly(lactic-co-glycolic acid) (PLGA) composite nanofibres, Chitosan-graft-PLGA (CS-graft-PLGA), produced by the electrospinning technique. CS was grafted onto the PLGA surface via the cross-linking agents reacting with the PLGA with reactive carboxyl groups on its surfaces introduced from the alkali treatment. The CS grafting ratios of the electrospun CS-graft-PLGA nanofibres were about 2.43%, 4.34%, 16.97% and 39.4% after cross-linked for 12 h, 16 h, 20 h and 24 h, respectively. The electrospun CS-graft-PLGA nanofibres were significantly uniform and highly smooth without the occurrence of bead defects, even at high CS grafting ratio. The electrospun CS-graft-PLGA nanofibres not only possessed the improved hydrophilicity and the protein absorption property, but also maintained the good mechanical property. In addition, the CS grafting can be conducive to accelerate degradation rate of PLGA.

1. Introduction

Electrospinning is a method of producing continuous fibres, the scale of which varies from several micrometers down to a few nanometers. Recently it has been widely used to fabricate a variety of polymer scaffolds consisting of the nano/microfibres for tissue engineering. Similar to the extracellular matrix (ECM), the obtained polymeric scaffolds own large surface area, high porosity and three-dimensional reticulate structures which are beneficial for improving the cells migration and proliferation onto the scaffolds [1–3]. So far a number of polymeric materials, such as poly(L-lactide) (PLA), poly(ε-caprolactone) (PCL), poly(lactic-co-glycolic acid) (PLGA), cellulose acetate (CA), polyvinyl acetate (PVA), poly(ethylene oxide) (PEO), chitosan, and collagen, had been successfully electrospun to nanofibres scaffolds [4–10]. However, these polymeric nanofibres scaffolds mentioned above are still not good enough to be applied in tissue engineering due to either poor mechanical properties, electrospinnability, processability of natural macromolecular polymers, or poor cell surface adherence of the hydrophobic surfaces of synthetic polymers. Thereafter, great efforts are contributed to fabricate the composite nanofibres scaffolds of the synthetic polymer and natural macromolecule via the electrospinning technique for better properties, such as PLGA/chitosan [11], PLGA/gelatin [12] and PLGA/collagen [13]. In addition, the surface modification of the electrospun synthetic polymer nanofibres using natural macromolecules has been investigated for applications in tissue engineering [14–17].

PLGA is one of the FDA-approved synthetic polymers as biomedical materials. It has excellent biocompatibility, tunable mechanical property and controllable degradation rate which can be achieved by regulating its crystal structure. Therefore it has been widely applied in biomedical field such as tissue engineering and drug delivery. However, the hydrophobicity of PLGA strongly affects the cell adhesion on the surface, so chitosan (CS), a natural polysaccharide with distinctive biological properties of good biocompatibility, biodegradability and wound healing acceleration, was mixed within PLGA solution and the PLGA/chitosan composite nanofibres was produced via the electrospinning technique in our previous work [18]. The improved cell adhesion on the surface of the PLGA/chitosan composite nanofibres was achieved at the cost of deteriorating mechanical properties. Moreover, the PLGA/chitosan mixture solution with high concentration of chitosan was too thick to be electrospun due to the high viscosity and strong hydrogen bonding [19–21]. In this study, a novel composite

* Corresponding author at: Center for Biomedical Materials and Engineering, Harbin Engineering University, No. 145, Na-Tong-Da Street, Nan-Gang District, Harbin 150001, China. Tel.: +86 451 8251 8644; fax: +86 451 8251 8644.
E-mail address: zhengwei75@126.com (W. Zheng).

0927-7765/$ – see front matter © 2012 Elsevier B.V. All rights reserved.
http://dx.doi.org/10.1016/j.colsurfb.2012.09.035

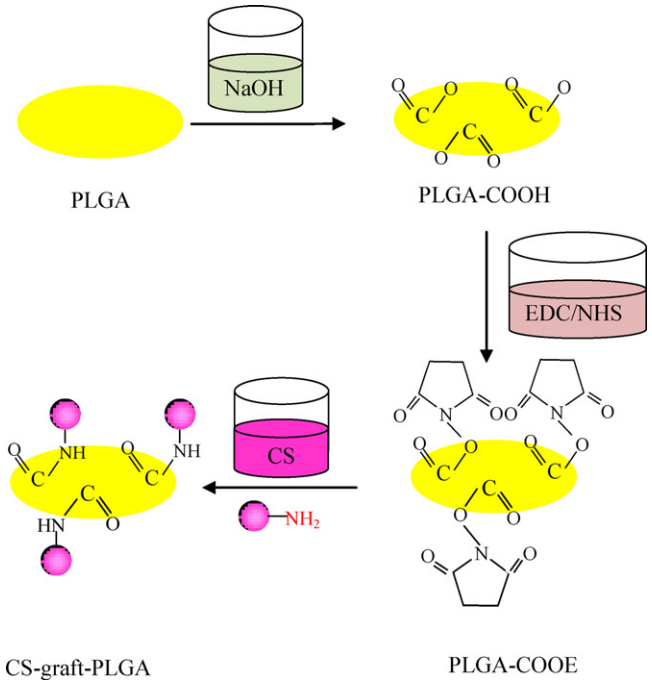

Scheme 1. Schematic illustration of the process of the CS grafting onto the PLGA surface.

of CS-graft-PLGA nanofibres is prepared via electrospinning technique with improved surface hydrophilicity and well maintained mechanical property.

2. Materials and methods

2.1. Materials

Poly(D,L-lactide-co-glycolide) (LA/GA 85/15, M_w = 200,000) was purchased from Jinan Daigang Biomaterial Co. Ltd. (China). Chitosan (CS, M_w = 1,000,000), dichloromethane (DCM), trifluoroacetic acid (TFA), 1-ethyl-3-(3-dimethyl-aminopropyl) carbodiimide hydrochloride (EDC) and *N*-hydroxysuccinamide (NHS) were purchased from Shanghai Aladdin Co. Ltd. (China). All chemicals were used directly without further purification. Aqueous solutions were prepared with doubly distilled water.

2.2. Preparation method

Preparation of the CS-graft-PLGA film: Firstly, 10 wt% solutions of PLGA in DCM were dried in air at room temperature. Then the solvent-casting PLGA films were soaked in 60 mg mL^{-1} NaOH aqueous solution for 1 h followed by thorough rinse using dilute hydrochloric acid and distilled water. Subsequently, the PLGA films were further immersed in a 10 mg mL^{-1} EDC/NHS solution for 6 h firstly and then transferred into the CS solution (25 mg mL^{-1}) and cross-linked for 12 h, 16 h, 20 h and 24 h, respectively. The preparation process is shown in Scheme 1. Finally, CS-graft-PLGA films were rinsed with distilled water and dried in vacuum at room temperature for 24 h.

Preparation of the CS-graft-PLGA nanofibres via the electrospinning method: the as-obtained CS-graft-PLGA film was completely dissolved in a mixture solvent of DCM/TFA (4/1 volume ratio) to prepare the 120 mg mL^{-1} electrospinning solution. The solution then was loaded into a plastic syringe equipped with a stainless-steel blunt needle of 0.5 mm in the outer diameter. The applied voltage was 9.5 kV supplied by a high voltage power supply (HB-F303-1-AC, China), the flow rate of the CS-graft-PLGA solution was 0.5 mL h^{-1} controlled by an infusion pump (TS2-60, Baoding Longer Precision Pump Co., China) and the distance between the tip of the needle and the product collector was 10 cm. For comparison, another two different types of CS and PLGA nanofibres were prepared as the following methods: Firstly, PLGA nanofibres were fabricated via the electrospinning technique and CS was modified on the electrospun PLGA nanofibres by soaking them in the CS solution for 12 h after surface treatment. The as-obtained PLGA nanofibres modified with CS is denoted as CS modified PLGA nanofibres. Secondly, the mixture of the CS solution and PLGA solution was electrospun under the same electrospinning conditions with CS-graft-PLGA nanofibres. The obtained electrospun nanofibres were denoted as PLGA/CS nanofibres. All samples were dried under vacuum at room temperature for 24 h.

2.3. Characterization

Attenuated total reflectance-Fourier transform infrared (ATR-FTIR) spectroscopic investigation was carried out on a Perkin-Elmer Spectrum One spectrophotometer (Perkin-Elmer Co., USA) for the chemical structure characterization of the CS-graft-PLGA films. The scanning range was 4000–650 cm^{-1} with a resolution of 4.0 cm^{-1} and 16 scans. X-ray photoelectron spectroscopy (XPS) analysis was performed using a Thermo Scientific K-Alpha ESCA instrument (Physical Electronic Co. PHI-5700, USA), which was equipped with aluminium Kα monochromatized radiation at 1486.6 eV. Spectra were recorded from 0 to 1350 eV for the binding energy, with a pass energy of 187 eV for the wide scan survey and a pass energy of 29 eV for the narrow scan survey of C 1s region. The amount of the grafted CS was measured via the thermogravimetric analysis (TGA, TA instruments Q-200, USA) from 20 to 700 °C at 20 °C/min heating rate and a nitrogen flow rate of 50 mL min^{-1}.

The morphologies of the electrospun CS-graft-PLGA nanofibres before and after biodegradation were observed by scanning electron microscope (SEM, FEI instruments Quanta 200, Holland). The diameter distribution of the nanofibres for each sample was also analyzed via the size measurement for at least one hundred nanofibres using Image J.

The hydrophilicity of the CS-graft-PLGA nanofibres was investigated by measuring water contact angles using water contact angle analyzer (FTA100, FTA Co., USA). The measurements were carried out at five different points on each sample surface.

The samples (approximately 10 cm^2) were incubated in the closed bottles containing 20 mL BSA solutions (1 mg mL^{-1}) at 37 °C. The absorbance of BSA solution was tested using UV-Vis spectrometer (Shimadzu UV-2550, Japan) at a wavelength of 280 nm for different incubation time periods.

The mechanical properties of the electrospun nanofibres were tested using Instron 3365 uniaxial testing machine with a 100 N load cell at 5 mm/min cross-head speed. All the testing specimens were cut into rectangular sheets with a size of 30 mm × 5 mm (gauge length 10 mm) and the thicknesses were accurately measured. Three specimens were tested for each type of the electrospun nanofibre samples.

For the in vitro degradation study, the electrospun nanofibres were accurately weighed after vacuum drying at room temperature for 24 h (W_0) and then incubated in closed bottles containing 10 mL phosphate buffer solution (pH 7.4) at 37 °C for up to 8 weeks. At weekly intervals the samples were accurately weighed again after deionised water rinse and vacuum drying for 48 h (W_t). The weight loss (%) was calculated according to the following equation:

$$\text{Weight loss}\ (\%) = \frac{W_0 - W_t}{W_0} \times 100$$

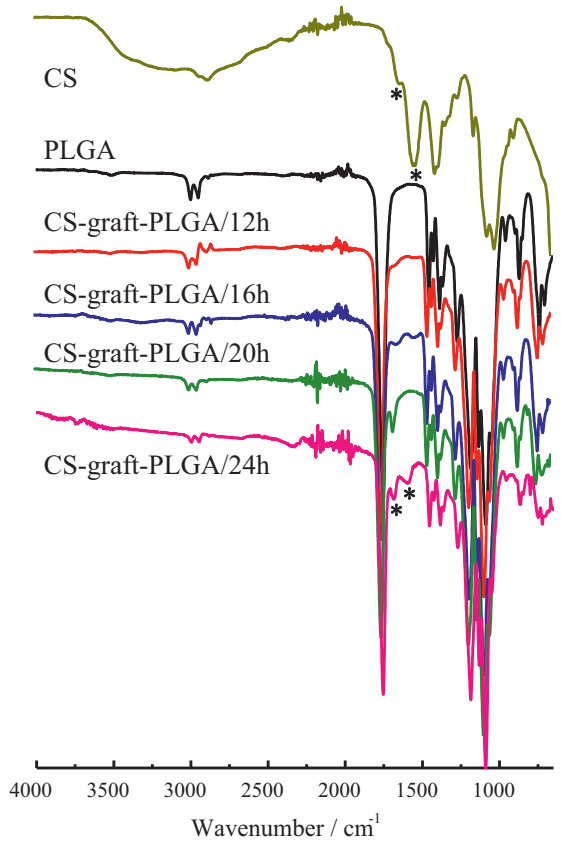

Fig. 1. FT-IR spectra of the CS films, the pure PLGA films and the CS-graft-PLGA films for different cross-link time.

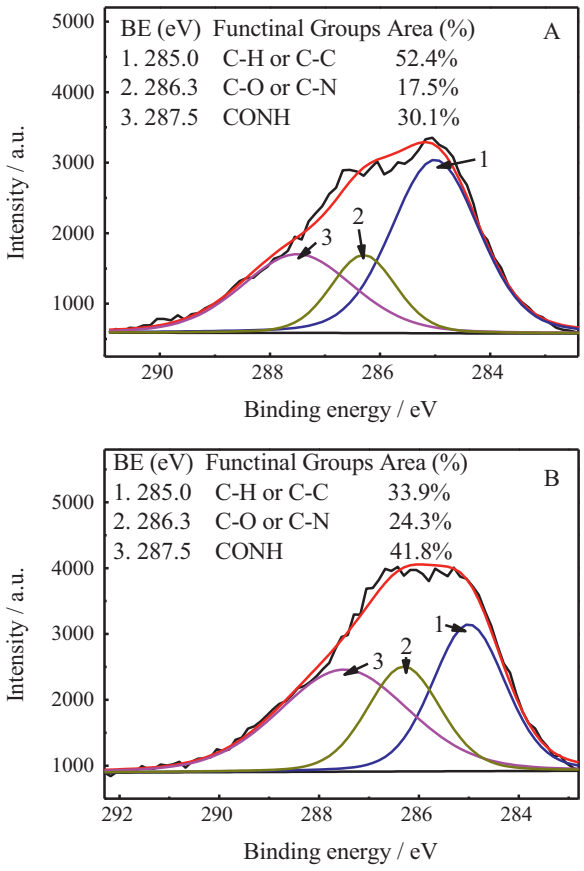

Fig. 2. XPS spectra of the CS-graft-PLGA films for different cross-link time: (A) 12 h and (B) 24 h.

The average value was taken from three measurements for each sample group. The morphological change after degradation was also studied by SEM.

3. Results and discussion

3.1. Characterization of the CS-graft-PLGA films

Fig. 1 shows the ATR-FTIR spectra of both the pure PLGA films and the CS-graft-PLGA films with different cross-link time. It can be seen that for the pure PLGA films the strong characteristic adsorption peaks at about 1752 cm^{-1}, 1452 cm^{-1}, 1182 cm^{-1} and 1130 cm^{-1} corresponded to carbonyl, C—O bond, C—O—C ether group and C—H methyl group, respectively. While for the CS-graft-PLGA films, besides the characteristic adsorption peaks of PLGA, the characteristic peaks of CS were also exhibited, the amide I at 1650 cm^{-1} and the amide II at 1540 cm^{-1} caused by C=O stretching vibrations and the combination of N—H in plane bending and C—N stretching vibrations, respectively [22,23]. Moreover, it also can be seen from the spectra that the CS characteristic bands (amide I and amide II) became more protruding with the increase of the cross-link time. Therefore, the FT-IR spectra suggest firstly that the CS had been successfully grafted onto the PLGA films and also the amount of the grafted CS depended on the cross-link reaction time. Furthermore, the results also indicates the amide bonds were formed when the CS was cross-linked onto the PLGA in the EDC/NHS solvent via reacting with the carboxyl groups after the PLGA was alkali treated (Scheme 1). In addition, a broad peak at 3420 cm^{-1} in the spectrum of the CS-graft-PLGA films was found which can be attributed to the stretching vibration of $-NH_2$, —OH, and intermolecular hydrogen bonding from CS [24].

Further characterization on the surface chemical structures of the CS-graft-PLGA films was conducted by XPS analysis. Fig. 2 shows the C 1s XPS region spectra collected from the surfaces of the CS-graft-PLGA films for different cross-link time. Three binding energy peaks at 285.0, 286.3 and 287.5 eV were observed in the C 1s region spectra of the CS-graft-PLGA films both cross-linking for 12 h (Fig. 2A) and for 24 h (Fig. 2B), which corresponded to C—C or C—H, C—O or C—N, and CONH, respectively. The peak at 287.5 eV was assigned to the amido bond, the characteristic peak of the CS, indicating that the CS has been grafted onto the PLGA films surface. Furthermore, the relative compositions for each peak based

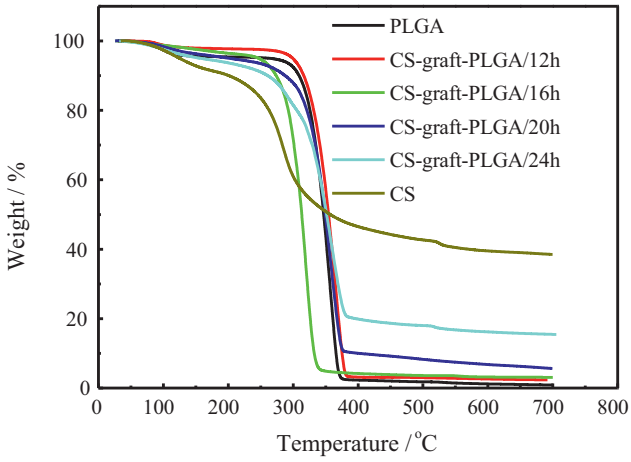

Fig. 3. TGA thermogram curves of the CS films, the pure PLGA films and the CS-graft-PLGA films for different cross-link times.

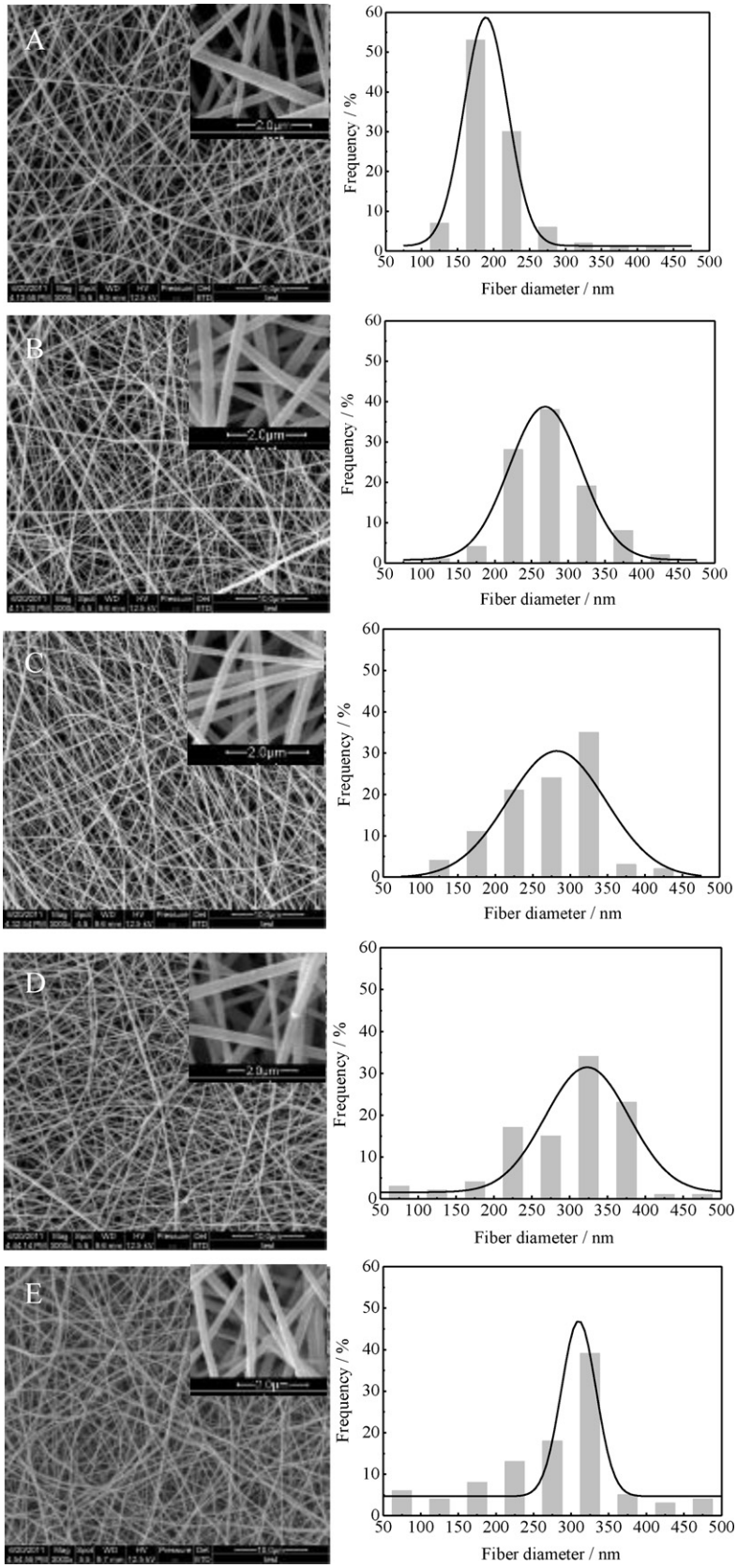

Fig. 4. SEM images of the electrospun pure PLGA (A) and the electrospun CS-graft-PLGA nanofibres for different cross-link times of 12 h (B), 16 h (C), 20 h (D) and 24 h (E) and their diameter distributions.

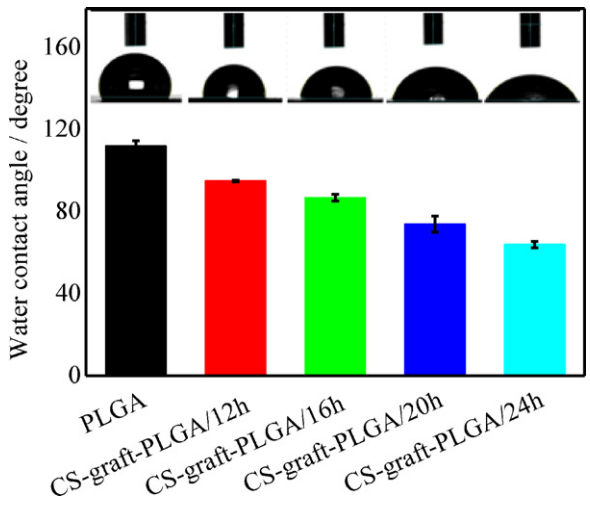

Fig. 5. Water contact angle results of the electrospun PLGA nanofibres and the electrospun CS-graft-PLGA nanofibres. Data are shown as mean ± SD ($n = 5$).

on area calculation were listed in the top-left corner in Fig. 2(A and B). It is evident that the relative composition for the CONH peak at 287.5 eV was 30.1% when the CS-graft-PLGA films was cross-linked for 12 h, lower than that of the CS-graft-PLGA films when cross-linked for 24 h (41.8%). This indicated that the amount of the grated CS on the PLGA films increased with the increase of the cross-link time.

Fig. 3 shows TGA thermogram curves of the CS-graft-PLGA films for different cross-link time periods. It is evident that the pure PLGA films started to degrade at around 280 °C and finished at about 370 °C with nearly 100% weight loss. On the other hand, the thermal degradation of the pure CS started at 220 °C and 51% weight was lost at around 370 °C. For the CS-graft-PLGA films, there was not much difference in the starting degradation temperatures, all were around 260 °C. However, the total weight losses of the CS-graft-PLGA films decreased with the increase of the cross-link time. The total weight losses were 96.94%, 96.13%, 90.81% and 81.33% for the CS-graft-PLGA films for cross-linking 12 h, 16 h, 20 h and 24 h, respectively. This is due to the increased amount of the CS grafted onto the PLGA surface with the prolonged cross-link time, thus the weight losses decreased when the CS-graft-PLGA films were heated up to 450 °C at which only the PLGA completely degraded and more CS was left. Therefore, the corresponding grafting ratios

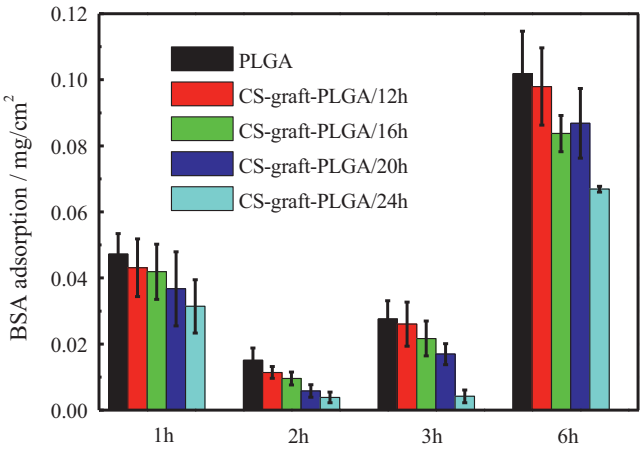

Fig. 6. Protein adsorption results of the electrospun PLGA nanofibres and the electrospun CS-graft-PLGA nanofibres. Data are shown as mean ± SD ($n = 3$).

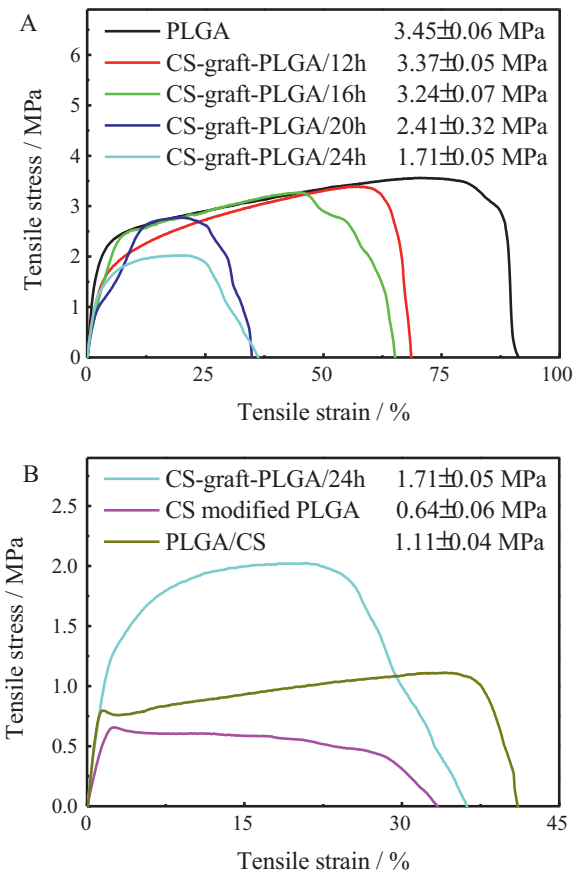

Fig. 7. Stress–strain curves of (A) the electrospun PLGA nanofibres and the electrospun CS-graft-PLGA nanofibres and (B) the electrospun CS-graft-PLGA nanofibres, CS modified PLGA nanofibres and electrospun CS/PLGA nanofibres.

for each type of the CS-graft-PLGA films can be calculated as 2.43%, 4.34%, 16.97% and 39.4%, respectively, according to the following equation:

$$\text{Grafting ratio } (\%) = \frac{\text{WL}_{\text{PLGA}}\ (\%) - \text{WL}_{\text{CS-graft-PLGA}}\ (\%)}{\text{WL}_{\text{CS}}\ (\%) - \text{WL}_{\text{CS-graft-PLGA}}\ (\%)}$$

WL, weight loss.

Clearly, the TGA results agreed very well with the ATR-FTIR and XPS results and analysis on the CS-graft-PLGA films.

3.2. Morphology of the electrospun CS-graft-PLGA nanofibres

Fig. 4 shows the typical morphology of the electrospun PLGA and CS-graft-PLGA nanofibres and their diameter distributions. It can be seen that the pure PLGA fibres and the CS-graft-PLGA fibres in nanoscale had been successfully produced using the electrospun technique. All the electrospun nanofibres were significantly uniform (as seen from the overview images in Fig. 4) and highly smooth without the occurrence of bead defects (as seen from the high magnification inset images in Fig. 4). However, the differences among the pure PLGA nanofibres and the CS-graft-PLGA nanofibres cross-linked for different time can be revealed by the diameter distribution histograms in Fig. 4. Compared to the pure PLGA nanofibres, the diameters of the CS-graft-PLGA nanofibres were larger and the diameter distributions were broader. Furthermore, the diameters of the CS-graft-PLGA nanofibres gradually increased and the diameter distributions broadened with the increase of cross-link time. The diameter of the electrospun nanofibres is affected by the applied electric voltage and the charge density of

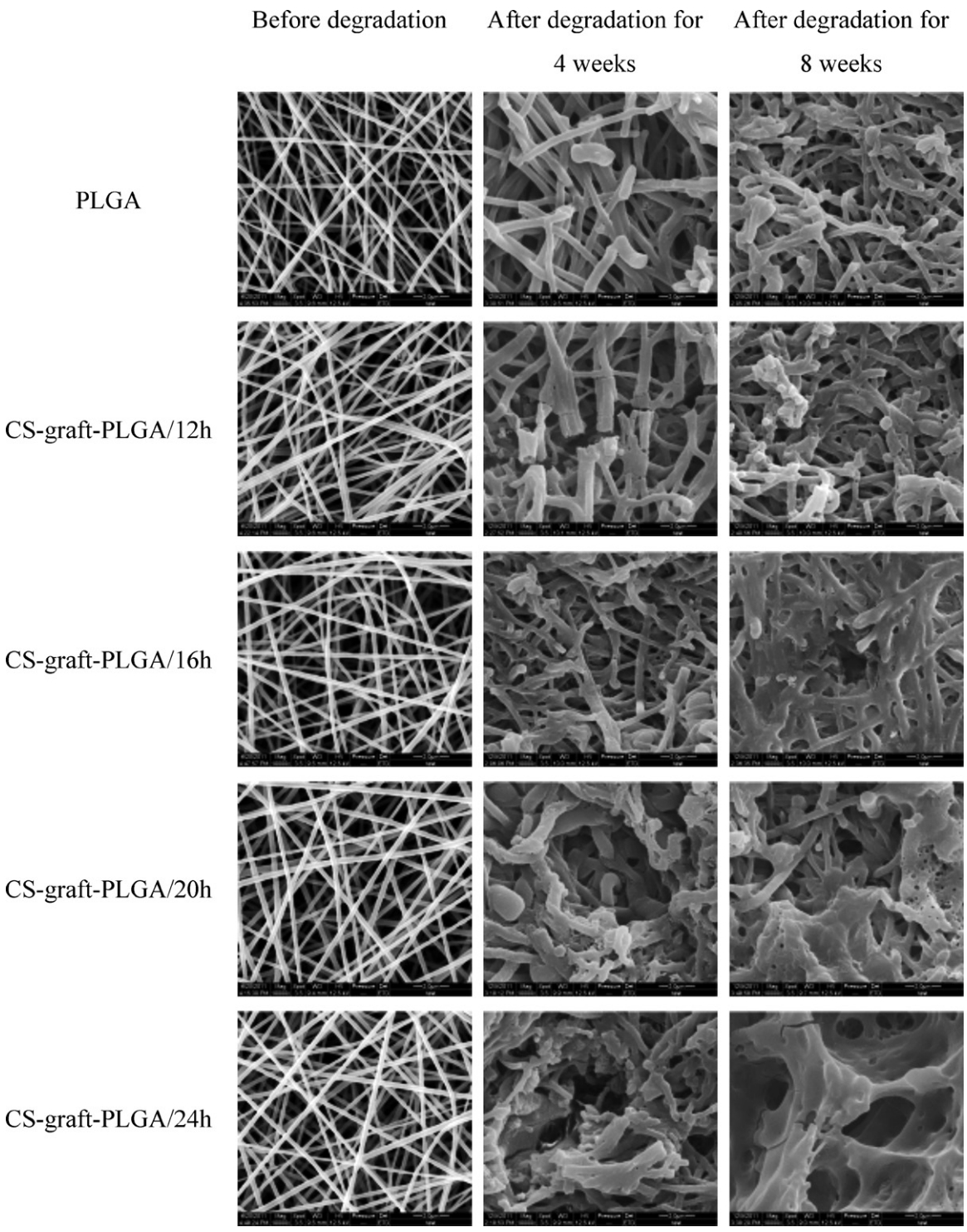

Fig. 8. Morphology evolution of the electrospun pure PLGA nanofibres and the electrospun CS-graft-PLGA nanofibres degraded in phosphate buffer solution (pH 7.4) at 37 °C for 4 weeks and 8 weeks.

polymer fluids which determines the electrostatic force and the surface tension, respectively. CS is an N-deacetylated product of chitin with positively charged polycation. However, amino groups of the CS react with the solvent of TFA to form salt resulting in the increase of charge density in polymer solution and thus the increase of the jet instability during electrospinning, therefore, the diameters of the resulting nanofibres were smaller. Furthermore, the increased amount of CS in the solution leads to the increase of the solution viscosity. As a result, higher surface tension due to the thicker polymer solution had to be overcome during the formation of nanofibres and the diameter distribution was broader. In addition, it should be stressed that the uniform and smooth CS-graft-PLGA nanofibres with as high as 39.4% grafted CS were successfully produced via the electrospin technique (Fig. 4E), while the surface quality of the CS/synthetic polymer fibres were very poor when CS concentration was high in previous reports [20,23,25–28].

3.3. Hydrophilicity of the electrospun CS-graft-PLGA nanofibres

The hydrophilicity is one of the most important surface characteristics of biomedical materials and it influences the protein absorption, the cell adhesion and proliferation, which could be determined by the chemical composition and physical structure of the material. Hence, we have investigated the influence of the CS amount on the hydrophilicity of the electrospun CS-graft-PLGA nanofibres. Fig. 5 shows the water contact angle variations of the electrospun PLGA nanofibres and CS-graft-PLGA nanofibres for different cross-link time. It can be seen that the water contact angles of the pure PLGA nanofibres was $111.97 \pm 2.59^{\circ}$, suggesting the hydrophobic surfaces of the pure PLGA nanofibres. However, after grafted CS onto PLGA, the water contact angles of the CS-graft-PLGA nanofibres were lower than that of the pure PLGA nanofibres. In addition, the water contact angles decreased from $95.01 \pm 0.43^{\circ}$ to $64.01 \pm 1.57^{\circ}$ with the increase of cross-link time due to the high grafting ratio of CS and a mass of amino and carboxyl groups on the surfaces of CS-graft-PLGA nanofibres. The difference of the water contact angles between the pure PLGA and CS-graft-PLGA nanofibres illustrated that the grafted CS improved the hydrophilicity of the PLGA nanofibres.

Fig. 6 shows the protein adsorption results of the pure PLGA nanofibres and the electrospun CS-graft-PLGA nanofibres. It was found that the adsorption amount of BSA firstly decreased and then increased with the increase of adsorption time for all nanofibres. This is because the desorption of the BSA protein was a rapid process when large amount of protein on the surface was adsorbed onto the nanofibres surfaces [29]. It is worth noting that the BSA adsorption amount on the CS-graft-PLGA nanofibres decreased with the increase of the CS grafting ratio. It also indicated that CS can improve the hydrophilicity of the PLGA nanofibres.

3.4. Mechanical properties of electrospun CS-graft-PLGA nanofibres

The stress–strain curves of the pure PLGA nanofibres and CS-graft-PLGA nanofibres are shown in Fig. 7A and the stress–strain curves of three types of the PLGA and CS composites are shown in Fig. 7B. It is evident that the tensile strengths of the electrospun CS-graft-PLGA nanofibres when cross-link time were 12 h and 16 h were equivalent to that of the pure PLGA nanofibres. The tensile strengths of the CS-graft-PLGA nanofibres for 12 h and 16 h's cross-linking were 3.37 ± 0.05 MPa and 3.24 ± 0.07 MPa, which is slightly lower than that of the pure PLGA nanofibres (3.45 ± 0.06 MPa). When cross-linked for 24 h, the tensile strength of the CS-graft-PLGA nanofibres (1.71 ± 0.05 MPa) sharply decreased to about 49% of the tensile strength of the pure PLGA nanofibres because of the high grafting ratio of CS. From Fig. 7B it can be seen that the tensile strength of the CS-graft-PLGA nanofibres with cross-link time of 24 h was apparently higher than that of the CS modified PLGA nanofibres (0.64 ± 0.06 MPa) and the electrospun PLGA/CS nanofibres (1.11 ± 0.04 MPa). Therefore, the tensile-tension results indicated that appropriate amount of CS grafted onto PLGA by cross-linking can maintain the good mechanical property of the PLGA nanofibres.

3.5. In vitro degradation of the electrospun CS-graft-PLGA nanofibres

The morphology changes of the electrospun nanofibres with the in vitro biodegradation time in phosphate buffer solution are shown in Fig. 8. After degraded for 4 weeks, each type of the electrospun nanofibres was swollen and congested together due to the chain relaxation of matrix polymers and a significant decrease in distance among the nanofibres. The pure PLGA nanofibres displayed the least morphological change and also the pure PLGA nanofibres remained stable after degradation up to 8 weeks. However, the short fibre fragments appeared for the CS-graft-PLGA nanofibres. Moreover, much more fibre collapse was observed for the CS-graft-PLGA nanofibres with increased CS content for the long time degradation. In addition, after degraded for 8 weeks, all the CS-graft-PLGA nanofibres showed significant conglutination and became harder and more brittle.

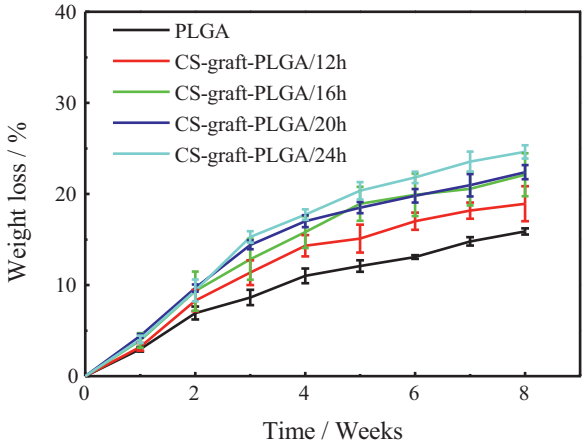

Fig. 9. Weight loss of the electrospun pure PLGA and the electrospun CS-graft-PLGA nanofibres at different degradation time points in phosphate buffer solution (pH 7.4) at 37 °C. Data are shown as mean ± SD ($n = 3$).

Fig. 9 shows the weight loss of the electrospun nanofibres with the in vitro degradation time in phosphate buffer solution for 8 weeks. It can be seen that the degradation rates of all nanofibres were rather high during the first 4 weeks and subsequently became steady for the following 4 weeks. Moreover, the CS-graft-PLGA nanofibres showed a larger weight loss than that of the pure PLGA nanofibres (about 15%). The weight loss was increased from 19% to 25% with the increase of the CS grafting ratio because CS degrades faster than PLGA. These results suggested that the grafted CS could be conducive for higher degradation rates of PLGA nanofibres.

4. Conclusions

In this study, a novel PLGA composite, CS-graft-PLGA nanofibres, is produced by electrospinning the CS-graft-PLGA composite solution. The CS was grafted onto PLGA surface via the two cross-link agents to react with the PLGA with reactive carboxyl groups on its surface after the alkali treatment. The grafting ratio of CS in the CS-graft-PLGA composite nanofibres can be up to 39.4% after cross-linked for 24 h. The electrospun CS-graft-PLGA nanofibres were significantly uniform and highly smooth without bead defects. The electrospun CS-graft-PLGA nanofibres possess better hydrophilicity with the higher CS grafting ratio. Good mechanical property of the pure PLGA nanofibres can be maintained with proper amount of grafted CS. In addition, the grafted CS can induce higher degradation rate of the PLGA nanofibres. These results are of importance to provide a new candidate for the novel tissue engineering scaffold.

Acknowledgements

This work is supported by the National Natural Science Foundation of China (Nos. 21275037 and 51201045), the Innovation Foundation of Harbin City (No. 2011RFQXS099), the Fundamental Research Funds for the Central Universities (Nos. HEUCFZ1123 and HEUCF201210008) and the Postdoctoral Science-Research Developmental Foundation of Heilongjiang Province (No. LBH-Q09131).

References

[1] E.S. Place, N.D. Evans, M.M. Stevens, Nat. Mater. 8 (2009) 457–470.
[2] Q.P. Pham, U. Sharma, A.G. Mikos, Tissue Eng. 12 (2006) 1197–1211.
[3] M.M. Stevens, J.H. George, Science 310 (2005) 1135–1138.
[4] S. Patel, K. Kurpinski, R. Quigle, H. Gao, B.S. Hsiao, M.M. Poo, S. Li, Nano Lett. 7 (2007) 2122–2128.
[5] J.M. Corey, D.Y. Lin, K.B. Mycek, Q. Chen, S. Samuel, E.L. Feldman, D.C. Martin, J. Biomed. Mater. Res. A 83 (2007) 636–645.
[6] S. Agarwal, J.H. Wendorff, A. Greiner, Adv. Mater. 21 (2009) 3343–3351.
[7] H.R. Pant, M.P. Neupane, B. Pant, G. Panthi, H. Oh, M.H. Lee, H.Y. Kim, Colloid Surf. B 88 (2011) 587–592.
[8] N. Krithica, V. Natarajan, B. Madhan, P.K. Sehgal, A.B. Mandal, Adv. Eng. Mater. 14 (2011) B149–B154.
[9] C. Cunha, S. Panseri, S. Antonini, Nanomed. Nanotechnol. 7 (2011) 50–59.
[10] W.I. Baek, H.R. Pant, K.T. Nam, R. Nirmala, H.J. Oh, I. Kim, H.Y. Kim, Carbohydr. Res. 346 (2011) 1956–1961.
[11] Z.X. Meng, W. Zheng, L. Li, Y.F. Zheng, Mater. Chem. Phys. 125 (2011) 606–611.
[12] Z.X. Meng, X.X. Xu, W. Zheng, H.M. Zhou, L. Li, Y.F. Zheng, X. Lou, Colloid Surf. B 84 (2011) 97–102.
[13] M.V. Jose, V. Thomas, D.R. Dean, E. Nyairo, Polymer 50 (2009) 3778–3785.
[14] W. He, Z.W. Ma, T. Yong, W.E. Teo, S. Ramakrishna, Biomaterials 26 (2005) 7606–7615.
[15] T.I. Croll, A.J. Connor, G.W. Stevens, J.J. Cooper-White, Biomacromolecules 5 (2004) 463–473.
[16] Y.B. Zhu, C.Y. Gao, X.Y. Liu, J.C. Shen, Biomacromolecules 3 (2002) 1312–1319.
[17] J.D. Schiffman, Y. Wang, E.P. Giannelis, M. Elimelech, Langmuir 27 (2011) 13159–13164.
[18] Z.X. Meng, Y.S. Wang, C. Ma, W. Zheng, L. Li, Y.F. Zheng, Mater. Sci. Eng. C 30 (2010) 1204–1210.
[19] P. Su, C. Wang, X. Yang, X. Chen, C. Gao, X. Feng, J. Chen, J. Ye, Z. Gou, Carbohydr. Polym. 84 (2011) 239–246.
[20] H. Homayoni, S.A.H. Ravandi, M. Valizadeh, Carbohydr. Polym. 77 (2009) 656–661.
[21] X.Y. Geng, O.H. Kwon, J.H. Jang, Biomaterials 26 (2005) 5427–5432.
[22] S.H. Lim, S.M. Hudson, Carbohydr. Polym. 339 (2004) 313–319.
[23] H. Deng, X. Li, B. Ding, Y. Du, G. Li, J. Yang, X. Hu, Carbohydr. Polym. 83 (2011) 973–978.
[24] J. Han, J. Zhang, R. Yin, G. Ma, D. Yang, J. Nie, Carbohydr. Polym. 83 (2011) 270–276.
[25] K. Desai, K. Kit, Polymer 49 (2008) 4046–4050.
[26] Z. Chen, X. Mo, F. Qing, Mater. Lett. 61 (2007) 3490–3494.
[27] S. Torres-Giner, M.J. Ocio, J.M. Lagaron, Carbohydr. Polym. 77 (2009) 261–266.
[28] J. Xu, J. Zhang, W. Gao, H. Liang, H. Wang, J. Li, Mater. Lett. 63 (2009) 658–660.
[29] W. Gao, B. Feng, Y. Ni, Y. Yang, X. Lu, J. Weng, Appl. Surf. Sci. 257 (2010) 538–546.